energies

MDPI

Technical Note

Toward the Application of Pulse Width Modulated (PWM) Inverter Drive-Based Electric Propulsion to Ice Capable Ships

Eric Christopher Renz [1] and James Turso [2,3,*]

[1] Ford Motor Company, Dearborn, MI 48126, USA
[2] Newport News Shipbuilding, Newport News, VA 23607, USA
[3] Department of Marine Engineering, United States Merchant Marine Academy, Kings Point, NY 11024, USA
* Correspondence: tursoja@email.gwu.edu

Abstract: The current world geopolitical state has driven significant interest in expanding influence in the polar regions. In order to develop new trade routes and defense of these areas, specialized ice-capable vessels are needed. Traditional propulsion technology utilized for these vessels has featured diesel and turbo electric drives with cycloconverter based technology used for speed regulation. Cycloconverter technology has the major disadvantage of characteristic output voltage waveforms that are very non-sinusoidal which induce harmonic rich currents with their resulting negative effects on total power factor and efficiency. There is also the potential to induce harmonic currents that may increase heat production in power cables, stressing insulation and reducing overall component life. Furthermore, sensitive loads such as control system power supplies may also be affected. The output waveform of a PWM drive has harmonic content that is both less severe, and more easily analyzed with current modeling tools. There are significant technical challenges that need to be assessed when considering PWM drive deployment in ice-capable vessels. This is due to the severe load torques, and torque variation imposed on propeller blades during ice-milling operations. To the authors' knowledge, an analysis of the behavior of vector-controlled PWM drives to this type of service has not been published in the open literature. This paper presents an initial modeling and simulation study that investigates whether such a PWM drive and associated controller may be effective for ice milling and other operational evolutions for these types of ships.

Keywords: ice breaker; PWM inverter electric drive; DQ control of propulsion motors

Citation: Renz, E.C.; Turso, J. Toward the Application of Pulse Width Modulated (PWM) Inverter Drive-Based Electric Propulsion to Ice Capable Ships. *Energies* **2022**, *15*, 8217. https://doi.org/10.3390/en15218217

Academic Editors: Lorand Szabo and Feng Chai

Received: 30 August 2022
Accepted: 31 October 2022
Published: 3 November 2022

1. Introduction

There are two general types of electric propulsion drive arrangements: dedicated and integrated. Dedicated systems are as the name implies, dedicated to propulsion needs only. Integrated systems serve all of the vessel loads, both propulsion and non-propulsion related. The key technical challenge for integrated systems comes from the need to control the speed of such a large electric load as a propulsion motor, while simultaneously providing constant and stable AC bus voltage, frequency, and low harmonic content. A typical AC/AC cycloconverter (CCV) system (Figure 1) includes multiple AC generators feeding a medium voltage bus. In the cycloconverter, the incoming voltage from each phase feeds a switched silicon-controlled rectifier (SCR) circuit. In so doing the frequency of the output voltage is varied. The output voltage wave form produced by cycloconverters is useful for propulsion, but is no longer a pure sinusoidal waveform. It becomes rich in harmonic content throughout the frequency spectrum such that tuned filters (harmonic trap filters) are ineffective in restoring power quality. The main method used to mitigate this phenomenon is the use of a 12 pulse cycloconverter circuit. This approach is accepted and has been adopted for ice-capable vessels.

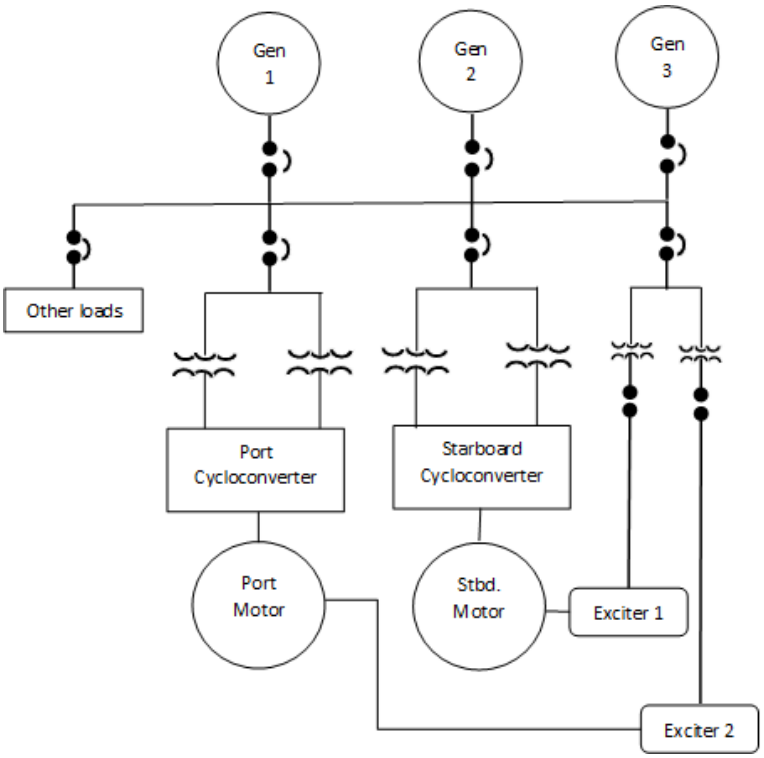

Figure 1. Typical Cycloconverter (CCV) System, [1] (p. 317).

The commercial availability of medium voltage Insulated Gate Bipolar Transistors (IGBT) and integrated gate-commutated thyristors (IGCT) has enabled the use of larger PWM motor drives needed for propulsion applications using induction motors and synchronous motors, including permanent magnet synchronous motors. The PWM drive is an AC/DC/AC technology. A typical 2-level drive topology is presented in Figure 2.

This type system needs more components than the AC/AC cycloconverter system described above. There are generators, a rectifier, a DC bridge that includes a filter/capacitor, and an inverter. The inverter is actively controlled to commutate the DC bridge voltage to a controlled waveform that consists of a series of rectangular pulses.

When applied to a sufficiently inducive load these pulses produce a current that is nearly sinusoidal, and consequently has a low harmonic content. The most effective way to control the pulsed waveform for a synchronous motor application is to commutate them to maximize torque for a given current. This results in greater overall efficiency of the PWM drive, and produces fuel savings which may justify the additional components and associated costs needed to make it work. While economic viability is of great importance for any new application of technology, the focus of this study considers only technical viability, with the hope that proven technical viability will be a natural precursor to consideration by industry including a conceptual design and economic viability study.

Large mechanical and electrical systems are expensive and complex. Performance testing can generate massive forces, with the potential to destroy the system itself if poorly designed. The objective of the system model is to emulate the performance of a real system, without having to build a prototype system. MATLAB/Simulink^{TM} is a tool that has been developed to model such complex systems.

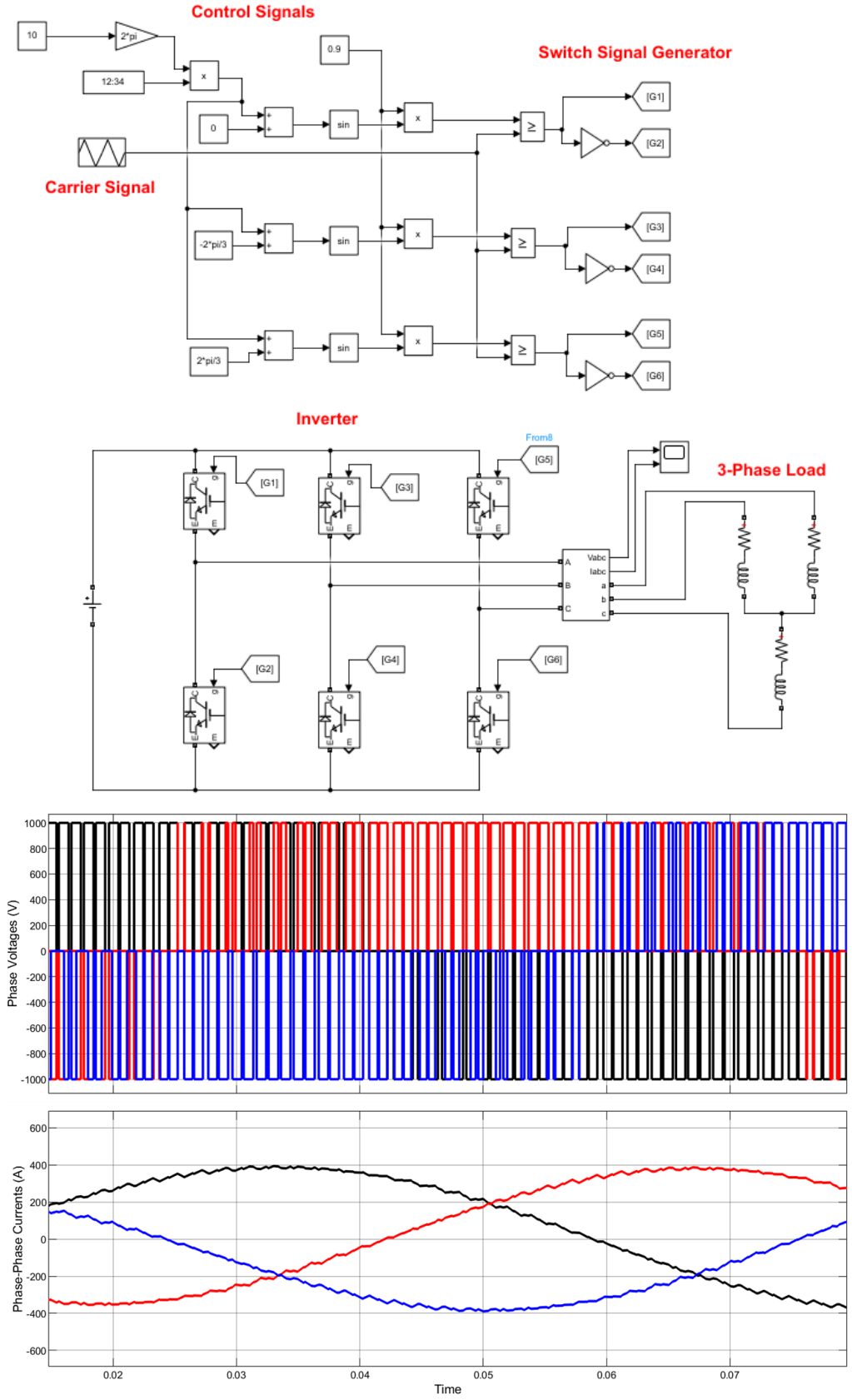

Figure 2. Typical PWM Inverter System and Output Waveforms.

2. Problem Description

The complex system chosen for this study is a functionally complete diesel electric marine power plant including generator speed control, voltage regulation, rectifier, DC link/filter, inverter, PWM drive controller, permanent magnet synchronous machine type propulsion motor, shaft, and propeller as shown in the following functional diagram (Figure 3). Dynamic modeling of the shaft dynamics, hull dynamics and propeller dynamics are based on the ice-capable vessel USCGC Healy.

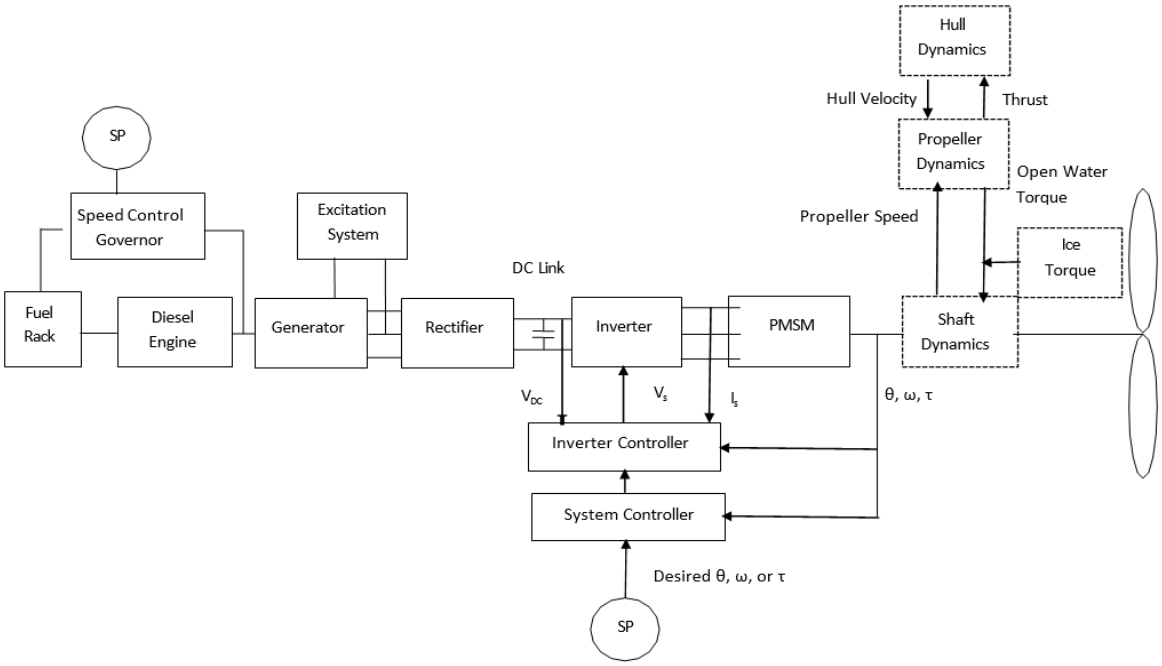

Figure 3. Functional Diagram of the Full System Model.

The USCGC Healy was chosen as the subject of study because it has an AC/AC cycloconverter drive which has been the subject of significant study in Reference [2] and has significant reference data available for comparison with a PMSM powered by a PWM drive system. Although the primary objective is to assess the ability of this type of system to sustain ice-milling torque (short term disruption), the author realizes that the model may be used to assess other, long-term events of potential significant interest. These include full system performance testing, such as an emergency astern test (e.g., "crash-back"). A permanent magnet synchronous motor model was chosen for the PWM model due to its being the technology of choice for modern marine propulsion systems and its simplicity and reliability due to it not requiring a separate excitation system. This has the added benefit of making the associated closed-loop space vector control system relatively straight-forward to implement, compared to comparably sized induction motor drive controllers. The entire power generation and propulsion drive system is modeled in Simulink^{TM}. The propulsion motor is modeled as a salient pole Permanent Magnet Synchronous Machine with five (5) pole pairs. The motor currently installed on USCGC Healy is a dual winding motor. The single winding motor model is effectively a proxy for one motor winding which serves one half of the external motor torque.

2.1. The Magnetic Flux Space Vector [2]

Consider a fixed stator with three coils installed 120 degrees apart. The three coils draw current which produce a magnetic field which depends on the magnitude and direction of the current. Given the three coils are fed from a balanced three-phase sinusoidal voltage

source, a current space vector, i_s, for a balanced 3-phase load with current amplitude I is defined as:

$$i_s = I\left[\cos(wt)e^0 + \cos\left(wt - \frac{2\pi}{3}\right)e^{-\frac{2\pi}{3}} + \cos\left(wt + \frac{2\pi}{3}\right)e^{+\frac{2\pi}{3}}\right]$$

The stator current space vector describes the equivalent current that would produce the same total magnetic field magnitude and direction as the three phase currents produce at a specified point in time [3]. By controlling the frequency and magnitude of individual currents to each phase, implicitly, the magnitude and direction of the resulting current space vector and internal magnetic field space vector, are also controlled. Spec vector control uses PWM motor control technology to dynamically position the flux vector within the PMSM, and can be used for speed, position, or direct torque control of the machine.

2.2. The D-Q Reference Frame [2]

The origin of the rotating current space vector is the motor rotational centerline, and is coincident with the origin of the direct-quadrature (D-Q) reference frame. The D-Q reference frame is fixed to the rotor, and rotates along with it. By adopting this reference frame, 3 phase quantities appear to be DC in steady-state, and are easier to control compared to their 3-phase counterparts. Indeed, use of a control system that manipulates motor winding voltage demand in the DQ reference frame enables a PMSM to be controlled as if it were a separately-excited DC motor. Figure 4 shows the DQ axes superimposed upon a (simplified) rotor permanent magnet. The permanent magnet flux vector is colinear with the D-axis.

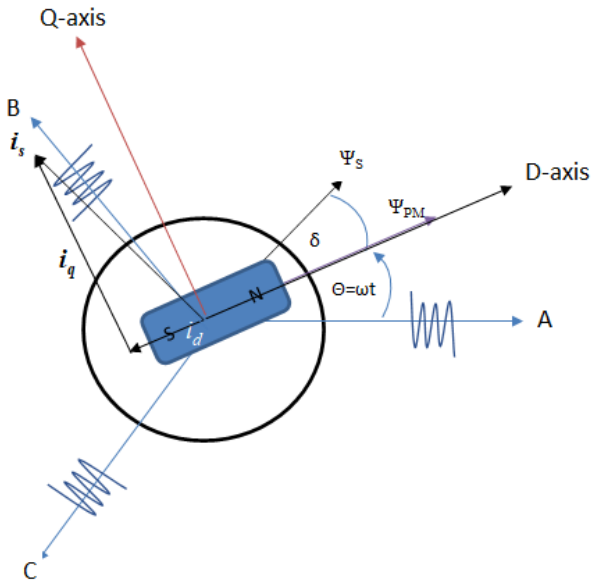

Figure 4. Rotor (i.e., DQ) Reference frame with current and flux vectors shown.

The transformation from the stationary ABC reference frame to the rotating (synchronous) DQ reference frame is provided in Equation (1).

$$x_{dq0} = \sqrt{\frac{2}{3}}\begin{bmatrix} cos(\theta) & cos\left(\theta - \frac{2\pi}{3}\right) & cos\left(\theta + \frac{2\pi}{3}\right) \\ -sin(\theta) & -sin\left(\theta - \frac{2\pi}{3}\right) & -sin\left(\theta + \frac{2\pi}{3}\right) \\ \sqrt{\frac{1}{2}} & \sqrt{\frac{1}{2}} & \sqrt{\frac{1}{2}} \end{bmatrix}\begin{bmatrix} a \\ b \\ c \end{bmatrix} \quad (1)$$

The transformation from the rotating (synchronous) DQ reference frame to the stationary ABC reference frame is provided in Equation (2).

$$x_{abc} = \sqrt{\frac{2}{3}} \begin{bmatrix} cos(\theta) & -sin(\theta) & \sqrt{\frac{1}{2}} \\ cos\left(\theta - \frac{2\pi}{3}\right) & -sin\left(\theta - \frac{2\pi}{3}\right) & \sqrt{\frac{1}{2}} \\ cos\left(\theta + \frac{2\pi}{3}\right) & -sin\left(\theta + \frac{2\pi}{3}\right) & \sqrt{\frac{1}{2}} \end{bmatrix} \begin{bmatrix} d \\ q \\ 0 \end{bmatrix} \quad (2)$$

The stator current space vector $i_{s,}$ can be thought of as the vector sum of the individual phase currents. The resulting magnetic field is shown as the stator field space vector, lagging the stator current space vector by 90 degrees. The stator current space vector can lead or lag the Q-axis. This would affect the power angle, which describes the angle difference between the rotor and stator flux vectors. The power angle δ dictates the mode of the synchronous machine (motor, δ lease the PM flux vector). The stator current space vector i_s can be decomposed into components i_d and i_q. If i_d is zero, then $i_s = i_q$. Given that the direct axis current is responsible for the rotor magnetic field, a permanent magnet machine requires no i_d.

As mentioned previously, the DQ transformation makes the 3-phase motor "appear" to be a DC motor from the perspective of the control system. With a PM motor, field current is unnecessary ($i_d = 0$) thus, the motor current is controlled by controlling i_q to some setpoint. For motor speed control, this setpoint would be provided by an outer speed control loop.

2.3. Voltage and Flux Linkage Equations [4]

The voltage equations of a PMSM given in the d-q rotor reference frame are provided below [2].

$$v_{sd} = R_s i_{sd} + \frac{d\psi_{sd}}{dt} - \omega\psi_{sq} \quad (3)$$

$$v_{sq} = R_s i_{sq} + \frac{d\psi_{sq}}{dt} + \omega\psi_{sd} \quad (4)$$

$$\psi_{sd} = L_{sd} i_{sd} + \psi_{PM} \quad (5)$$

$$\psi_{sq} = L_{sq} i_{sq} \quad (6)$$

For modeling of the Healy's PMSM, these equations are implemented in a Simulink™ Simscape™ Permanent Magnet Machine block.

2.4. PMSM Model Parameters

PMSM model parameters include the flux of the permanent magnet, reference currents, torque constant, and motor winding impedances. The motor winding impedance values were based on those given in Reference [3]:

$$L_d = 0.0298\ H$$

$$L_q = 0.0159\ H$$

$$R_S = 0.0133\ \Omega$$

According to [3], the USCGC Healy has two 15,000 HP dual winding propulsion motors. The Simulink™ platform supports a single winding PMSM only, so it was instead modeled as a single 7500 HP (5593 kW) motor with an associated scalar multiplier (2) used to adjust performance for the full 15,000 HP per propulsion shaft. The motor torque is proportional to the rated power at rated shaft speed as follows:

$$T = \frac{P}{160RPM * (2\pi/60)} = 3338008\ N - m \quad (7)$$

where: T = Torque, Newton-meters. P = Power, (5,593,000 Watts)

The Delta-connected motor winding voltage at full power is 2320 $Vrms_{,\,L–N}$. The corresponding line current at rated power factor (0.7)

$$Power = 3 * V_{LN} I_{line} * \ Power\ Factor \tag{8}$$

$$I_{line} = \frac{P}{3 * V_{LN} * PF} = 1194\ A \tag{9}$$

where: I_{line} = Line current, Amperes. P = Power, (5,593,000 Watts). PF = power factor (0.7)

The motor torque constant may be calculated now as the ratio of rated torque to peak current is known.

$$Torque\ Constant = \frac{T}{3 * I_{LN}} = 93.2\ N - m/Amp \tag{10}$$

where: T = Torque, (333,800 Newton-meters). I_{LN} = Line current, (1194 Amperes).

Motor torque for a PMSM can be characterized according to the following equation [4]:

$$T_e = \frac{3}{2} p \left[\psi_{PM} i_{sq} - \left(L_{mq} - L_{md} \right) i_{sq} i_{sd} \right] \tag{11}$$

For a surface mounted PMSM, L_{mq} and L_{md} are nearly equal. PMSM motors generally do not have damper coils in them, therefore i_d = 0. As i_d is controlled to zero as well, the above torque formula is simplified to:

$$T_e = \frac{3}{2} p \left[\psi_{PM} i_{sq} \right] \tag{12}$$

This relationship can be used to calculate the current reference values for the PMSM model. Since the current reference has been calculated already, as well as the torque, the required flux of the permanent magnet can be calculated as follows:

$$\psi_{PM} = \frac{2 * T_e}{3 * p * \sqrt{2}\, i_{sq}} = 26.3\ \text{Webber} \tag{13}$$

where: ψ_{PM} = magnetic flux, Webber. T_e = Torque, (333,800 Newton-meters). p = number of poles (5). i_{sq} = q component current, (1194 Amperes)

The number of pole pairs and the magnetic flux linkage of the permanent magnet are constant values, thus, with i_d = 0, the electromagnetic torque is directly proportional to i_{sq}, in effect having a 3-phase permanent magnet synchronous motor appear as a separately-excited DC motor (to the control system), with the amount of torque directly proportional to the magnitude of the stator current space vector, i_{sq} applied to it (as presented in Equation (12)).

The control method for the PMSM needs to control i_q for torque production and $i_d = 0$ (or as close to it as possible during transient), regardless of the potentially massive and sudden external torque loads which may be encountered during ice-capable service. The control method requires rotor position (as measured by an encoder) to be relayed constantly to the controller, where field commutation is adjusted continuously. For ice capable vessels, external torque loads encountered during ice milling are a concern because these external forces are relatively large, intermittent, and repetitive. To the authors' knowledge, an analysis of the behavior of vector-controlled PWM drives for this type of service has not been published in the open literature. These forces act to disturb the rotor position, knowledge of which is critical to successful application of the vector control method—this analysis seeks to investigate the effects of these disturbance torques on the closed-loop behavior of the system.

2.5. Motor Control System Overview

The system is based on speed control—the desired propulsion shaft speed is input as a throttle command to a cascaded current control loop, where an outer PI controlled speed loop provides a Q-axis current demand signal. The output of the inner current loop is inverter output voltage demand to the inverter, where the inverter output voltage across the motor stator windings modulates the stator current space vector as required to increase or reduce motor torque as necessary to match the desired shaft speed. There are several other sub-systems that support this action and are necessary to make it work properly. The stator current space vector is the vector sum of the individual phase currents at any given time. The magnitude and the phase of these field currents are controlled by controlling the magnitude and phase of the voltage supplied to the stator windings. i_d is not a measured quantity that is available directly from measurements, therefore the 3-phase currents must be measured and transformed to the dq reference frame. Both the D-axis and Q-axis currents are controlled using Proportional-plus-Integral (PI) controllers with the D-axis current demand being equal to zero. It was found during the analysis that acceptable demand following and disturbance rejection were achieved using PI controller with proportional and integral gains (respectively) K_p = 6000 and K_i = 1000. These values were determined via iterative testing and successive tuning, given that inner current loop gains are typically orders of magnitudes higher than speed control gains due to the system electrical dynamics responding mush faster than the mechanical characteristics (e.g., mechanical inertia), making the current response is virtually instantaneous compared to the system's mechanical response. Figure 5 presents the flux vector controller implemented in Simulink™. The voltage demands calculated for the d and q axes are in-turn inverse transformed to the abc reference frame, normalized to the value of the DC link voltage, and converted to logic signals used to actuate the IGBT switches in the inverter. Figure 2 illustrates the process of generating switch signals from a demand signal. The control voltages would be generated from the inverse-transformed d and q axis demand signals from the control system shown in Figure 5.

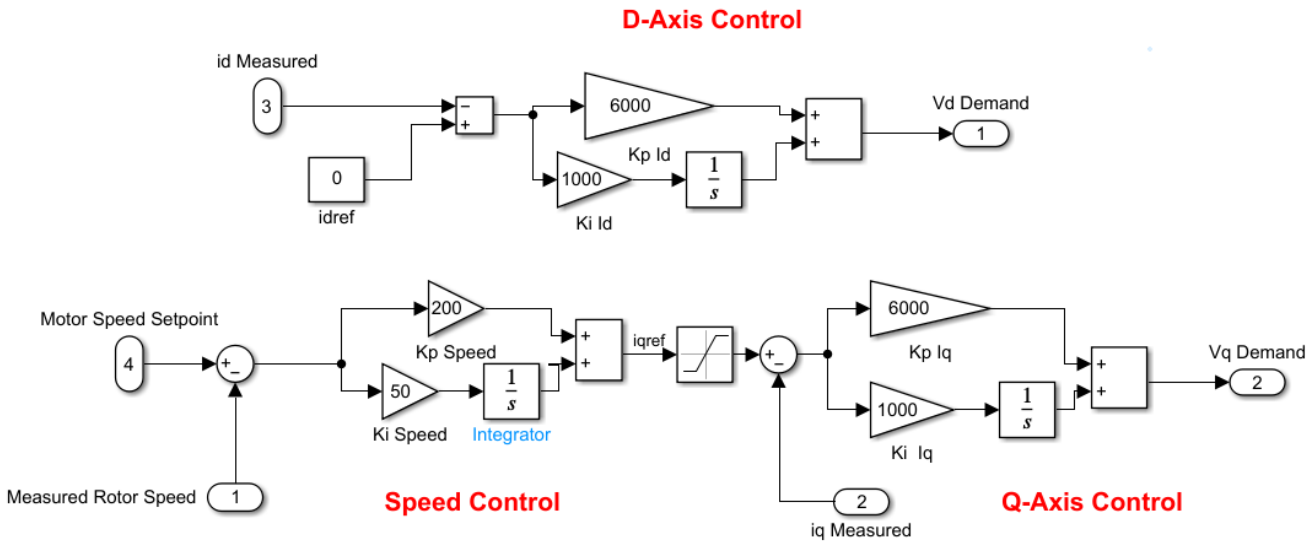

Figure 5. Cascade control of PMSM current.

2.6. USCGC Healy Simulink Model

The main objective of the study is to verify the stability of the controlled system during a variety of operational scenarios encountered by ice-capable ships. This model would be considered an end-to-end model in that the Diesel generator through propellor has been modeled to varying degrees of complexity consistent with the goals and objectives of this study. The model developed supports analysis of the impact of propulsion motor loads

on a theoretical shared electric distribution system and identify and quantify potential impacts to power quality by the PWM drive, if any. Figures 6 and 7 present the end-to-end Simulink^{TM} model used for this analysis.

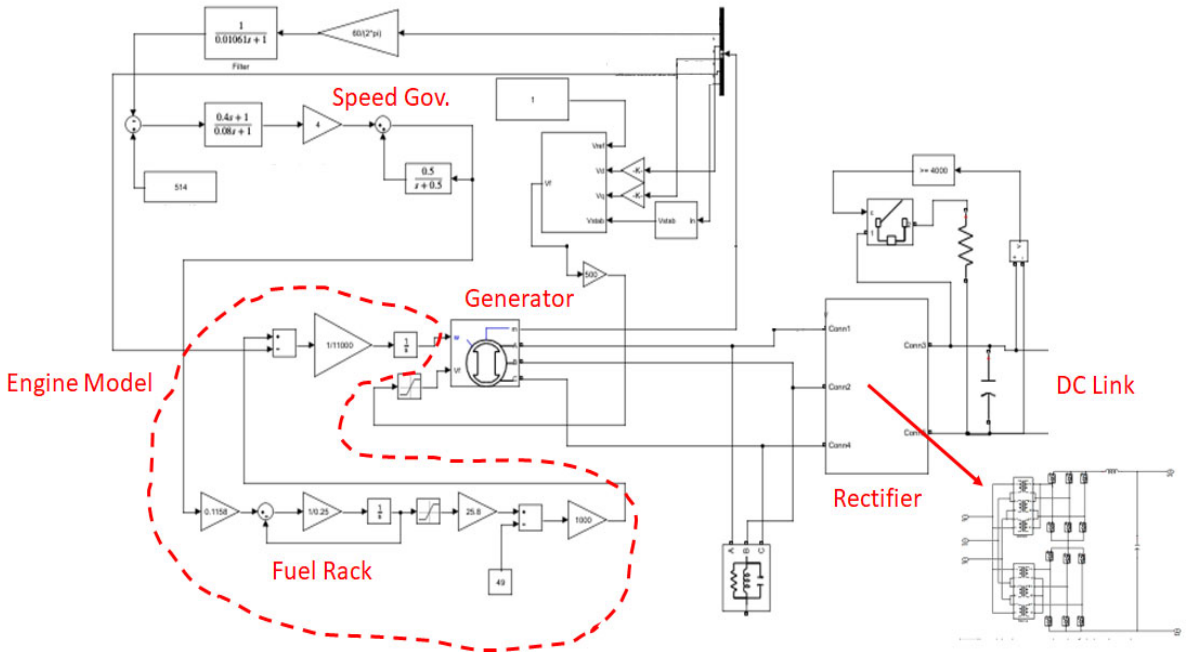

Figure 6. Diesel Engine/Generator/Rectifier Simulink^{TM} Model.

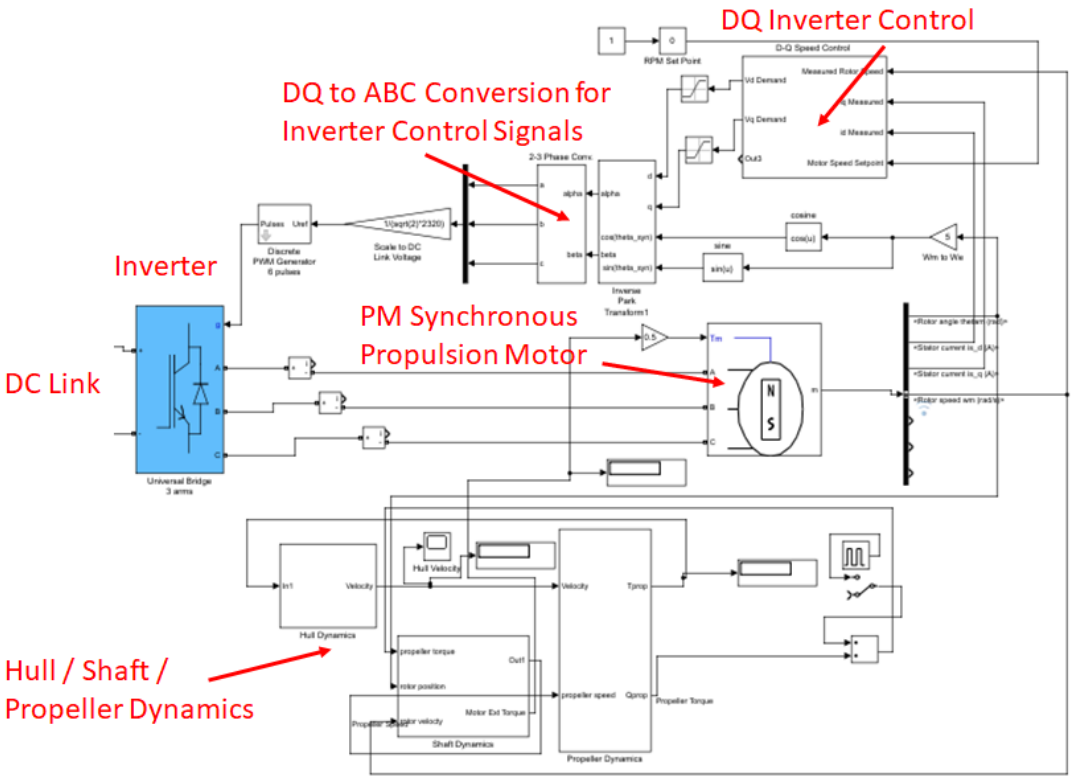

Figure 7. DQ Controller/Inverter/Propulsion Simulink^{TM} Model.

2.7. Engine/Generator

The generator model is modeled as a diesel driven synchronous machine with the properties inspired from the USCGC Healy—four 7.2 MW, 6.6 kV, 0.7 power factor, three-phase, 514 RPM engines as documented in Reference [2].

The engine is modeled as a first-order system, where engine acceleration is function of the net total torque of the engine/generator system divided by the inertia of the rotating assembly.

$$\dot{\omega}_{engine} = \left(Q_{engine} - Q_{generator}\right) / J_{total} \tag{14}$$

The engine torque ultimately is proportional to the fuel rack position and any first order lags associated with the turbocharger dynamics. Generator electrical torque due to load are calculated using a wound-field synchronous generator Simulink model, using standard impedance consistent with a machine of its size. The angular acceleration value from this subsystem is integrated to obtain the rotor speed of the Diesel engine/synchronous generator assembly.

Reference [2] included a functional diagram of the engine speed control governor system including proportional and integral gains, a speed signal filter, and actuator both with respective first order time constants. As originally modeled a dual proportional gain was included. This approach was abandoned and a single proportional gain was used to promote better stability in the new end-to-end model.

A separate (non-engine driven) excitation system was modeled after the IEEE Type 1 Synchronous Machine Voltage Regulator Model. Although shaft-driven DG generator type excitation systems are still in use, modern practice has favored separate, solid state excitation systems. This approach has the added benefit of decreasing complexity of the model while mimicking likely system performance.

2.8. Rectifier Circuit & DC Link/Filter

A 12-pulse type rectifier circuit was selected (instead of 6-pulse or 24 pulse) as typical AC/DC conversion technology used for PWM motor drive applications. The multi-pulse rectifier provides for lower harmonic content in the AC system upstream of the rectifiers. Parallel delta-wye and delta-delta transformers were used. A line inductor of 0.002 H was found to provide adequate performance with low voltage ripple. The DC link is fitted with a 0.005 F capacitor. All of these values were iteratively adjusted to get acceptable system dynamic and harmonic performance.

2.9. Inverter/Motor Drive

The inverter used for this study is a 2-level, 6 device (IGBT) inverter, fed from the DC link. The DC link provides a relatively smooth DC voltage at the approximately the line-to-line peak voltage of the generator output. Using sine-triangle pulse-width modulation (SPWM—shown in Figure 2), the output from the dq current controller to converted to the abc reference frame, as a control signal. The control signal is normalized to the DC voltage and compared to a triangle wave generated at a designated switching frequency. As shown in Figure 2, the normalized control signal and triangle wave are logically compared, with the output of the comparison being the IGBT actuation signal (conduct or not). The motor windings are powered by the pulse-width-modulated inverter output voltage.

2.10. Hull Characteristics/Propellor Shaft Dynamics

A traditional marine AC power generation and PWM drive system seldom experiences transient load events imposed on an ice-capable ships. Accordingly, additional models must be included that describe the dynamics of the propeller, shaft, and hull subject to external forces that impose a time-varying load torque on the propulsion motor. The equations describing hull characteristics and propellor shaft dynamics used for this study were derived from Reference [2].

2.11. Hull Dynamics

The hull dynamics model is based on linear (ahead and astern) motion only where the acceleration of the ship mass is determined by the net thrust divided by the vessel mass in accordance with Newton's second law of motion:

$$F_{net} = M \times \dot{V} \tag{15}$$

$$F_{net} = F_{eff} - R_T \tag{16}$$

$$F_{eff} = N_{prop} \times F_{prop} \times (1 - t) \tag{17}$$

where: F_{net} = net force (fore and aft) on the vessel, Newtons. F_{eff} = effective total propeller thrust, Newtons. F_{prop} = propeller thrust of each propeller, Newtons. N = number of propellers. t = thrust reduction fraction (dimensionless). R_T = total hull resistance, Newtons. M = effective vessel mass, kg. $\dot{V}$= vessel acceleration.

The thrust reduction fraction, t, typically ranges from 0.1 to 0.2 for twin propellor shaft ships, with the larger value typical for ships with bossings [5]. A value of 0.2 was included the model. The design displacement was assumed to be 16,000 LT [2]. The hull resistance, R_T, is different depending on whether the vessel is in open water or ice.

Figure 8 shows the hull dynamics model. The resistance model may use either ice breaking resistance or open water resistance but not both concurrently.

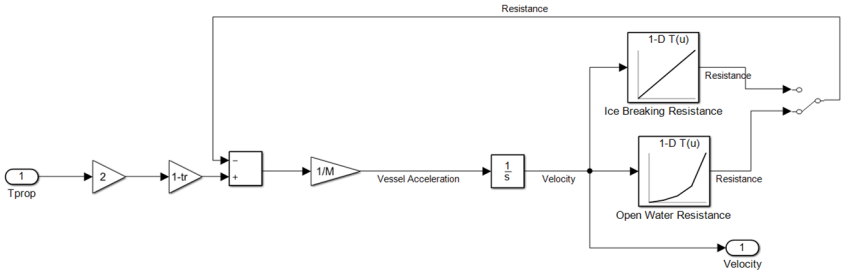

Figure 8. Hull dynamics model implemented in Simulink™.

2.12. Hydrodynamic Resistance

Both open water hull resistance and ice-braking resistance must be considered. Reference [3] provided typical curves for each of these cases (Figure 9). These curves were approximated in the Simulink model using lookup tables.

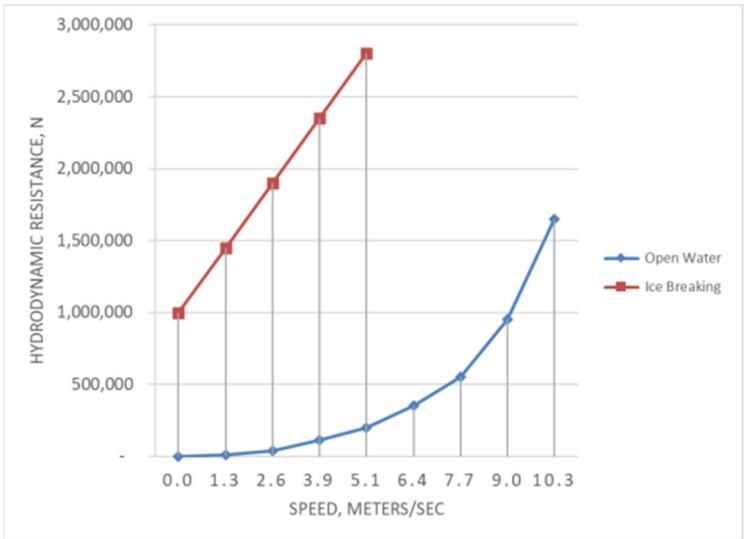

Figure 9. Hull resistance curves.

2.13. Shaft & Propeller Dynamics

The propulsion shaft (Figure 10) is a complex mechanical system that has many forces acting on it together. Reviewed in order from the motor outboard end to the stern tube bearing, the motor windings provide electromechanical torque that varies with the magnitude of the current space vector.

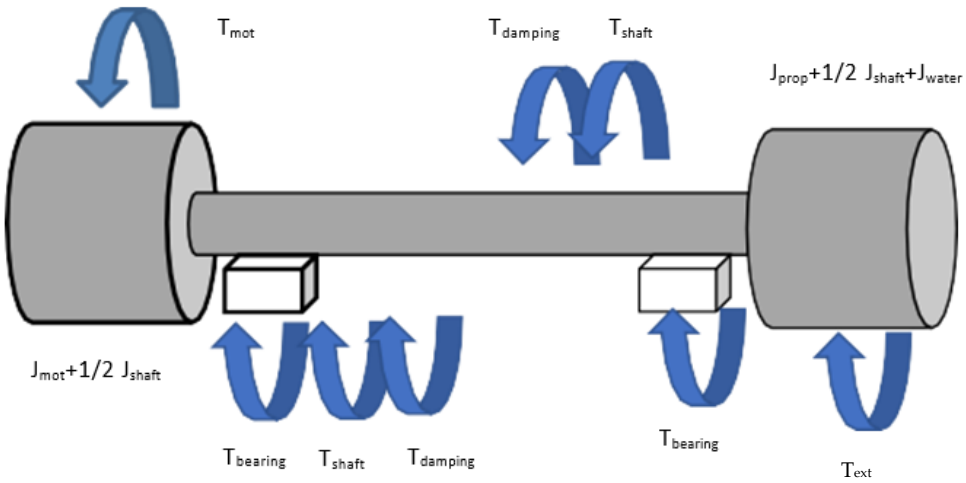

Figure 10. Shaft dynamics diagram.

Opposing this motor torque is the inertia of the rotor and shaft, motor bearing friction, shaft elastic torque, and internal shaft damping torque.

From the propeller end there is the shaft torque plus the damping force less the stern tube bearing friction, inertia of the shaft, including the propeller and entrained water, and finally the external torque from the hydrodynamic resistance. If the vessel is in ice, then the propeller is also subject to external torque loads from impacting the ice.

The propulsion shaft system model is best represented visually:

The sum of the torques on the motor side of the line shaft may be represented mathematically as follows:

$$T_{mot} - \left(J_{mot} + \frac{1}{2}\,J_{shaft}\right)\ddot{\theta}_m - D_{brg}\dot{\theta}_m - \left(\dot{\theta}_m - \dot{\theta}_p\right)C_{shaft} - \left(\theta_m - \theta_p\right)K_{shaft} \quad (18)$$

$$\left(\theta_m - \theta_p\right)K_{shaft} - \left(J_{prop} + J_{water} + \frac{1}{2}\,J_{shaft}\right)\ddot{\theta}_p - D_{brg}\dot{\theta}_p + \left(\dot{\theta}_m - \dot{\theta}_p\right)C_{shaft} - T_{ext} \quad (19)$$

where: C_{shaft} = Internal damping coefficient, 71.4 kN-m-s/rad, per Reference [3]. K_{shaft} = Shaft torque coefficient, 112 MN-m/rad, per Reference [3]. D_{brg} = Bearing coefficient of friction, 500 kN-m-s/rad, assumed for both motor and stern tube bearings. T_{mot} = Motor electromagnetic torque, N-m, variable. T_{ext} = Propeller external torque, N-m, variable. J_{mot} = Motor moment of inertia, 18,100 kg-m^2, per Reference [3]. J_{shaft} = Shaft moment of inertia, 18,100 kg-m^2, per Reference [2]. J_{prop} = Propeller moment of inertia, 41,200 kg-m^2, per Reference [2]. J_{water} = Entrained water moment of inertia, 5100 kg-m^2, per Reference [3]. $\ddot{\theta}_m$ Motor end angular acceleration, rad/s^2. $\dot{\theta}_m$ = Motor end angular velocity, rad/s. θ_m = Motor end rotor angular position, rad. $\ddot{\theta}_p$ = Propeller angular acceleration, rad/s^2. $\dot{\theta}_p$ = Propeller angular velocity, rad/s. θ_p = Propeller angular position, rad.

The PMSM Simulink^{TM} block uses load torque calculated from the model above and calculates rotor speed and angular position. The shaft model sums the external and internal system torques into a total motor external torque that is experienced by the propulsion motor. Since only one 3-phase set of windings of the propulsion motor is modeled, only one half of the shaft torque is used as the total external torque input to the PMSM model.

2.14. Hydrodynamic Propeller Torque and Thrust

The hydrodynamic propeller torque is the torque developed due to the reaction of the propeller blades relative to their relative motion with respect to the surrounding water. This torque is a function of the water density, propeller rational speed, propeller diameter, relative rotational efficiency, and vessel velocity. The propeller thrust is a function of these same quantities less the relative rotative efficiency.

These quantities are related according to the following per Reference [3]:

$$Propeller\ Torque = T_{prop} = C_Q \rho D^3 \left(V_A^2 + n^2 D^2\right) / \eta_R \tag{20}$$

$$Propeller\ Thrust\ Force = F_{prop} = C_T \rho D^2 \left(V_A^2 + n^2 D^2\right) \tag{21}$$

$$Apparent\ Velocity\ of\ Ship = V_A = V(1 - w_t) \tag{22}$$

$$Advance\ Coefficent = U = nD / \left(V_A^2 + n^2 D^2\right)^{1/2} \tag{23}$$

where: T_{prop} = *Propeller torque*, N-m. F_{prop} = *Propeller thrust force*, N. ρ = Density of seawater, kg/m^3. n = Propeller speed, revolutions/s. D = Propeller diameter, m. η_R = relative rotative efficiency, percent. V_A = Apparent hull velocity, m/s. V = Hull velocity, m/s. w_T = Effective Tailor wake fraction based on thrust identity. Percent. U = Advance coefficient, calculated. C_Q = Torque coefficient, dimensionless. C_T = Thrust coefficient, dimensionless.

Reference [3] uses a technique that indexes C_T (Figure 11) and C_Q (Figure 12) directly as a function of U. This method is very efficient for modelling and was incorporated into the model in the form of lookup tables that are switched on depending propulsion mode (forward or reverse) and hull velocity. By using this same technique, it is possible to compare performance cases for the PWM drive with the AC/AC drive model used in Reference [2].

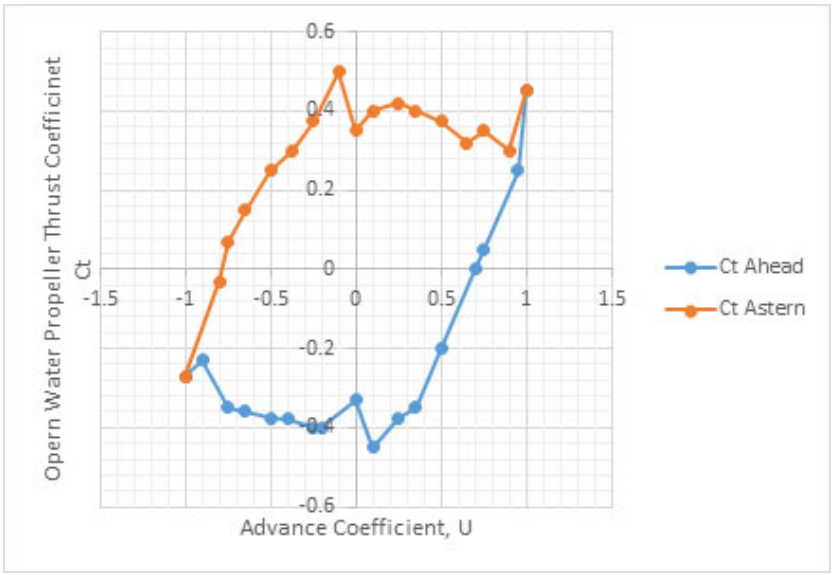

Figure 11. Shaft thrust coefficient vs. advance coefficient.

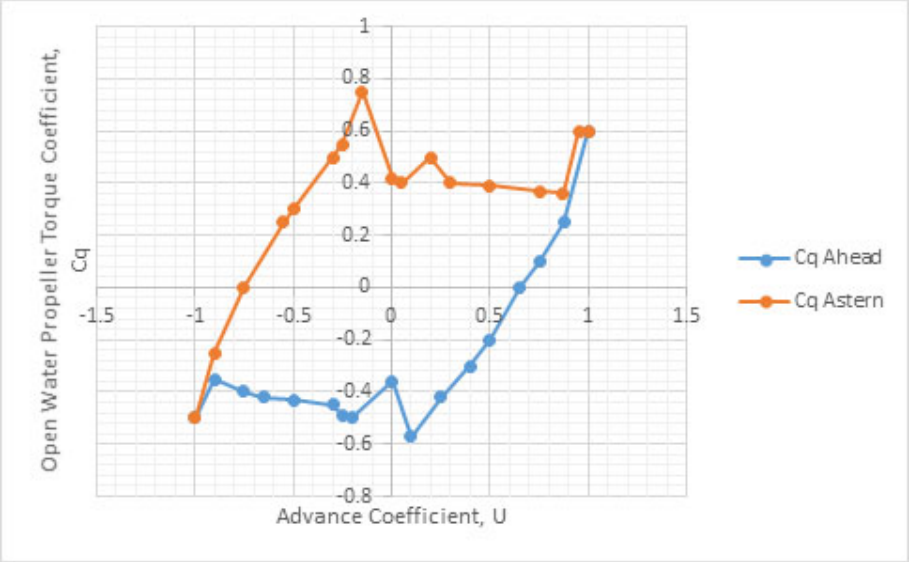

Figure 12. Shaft torque coefficient vs. advance coefficient.

2.15. Ice Milling Torque

The torque model employed in Reference [3] is a series of steep triangular spikes with a peak magnitude of 1540 kN-m based on MARITECH Report No. 82-116 (1982).

These spikes are modeled as four equidistant pulses per revolution to coincide with the four propeller blades. The corresponding Simulink model is shown in Figure 13.

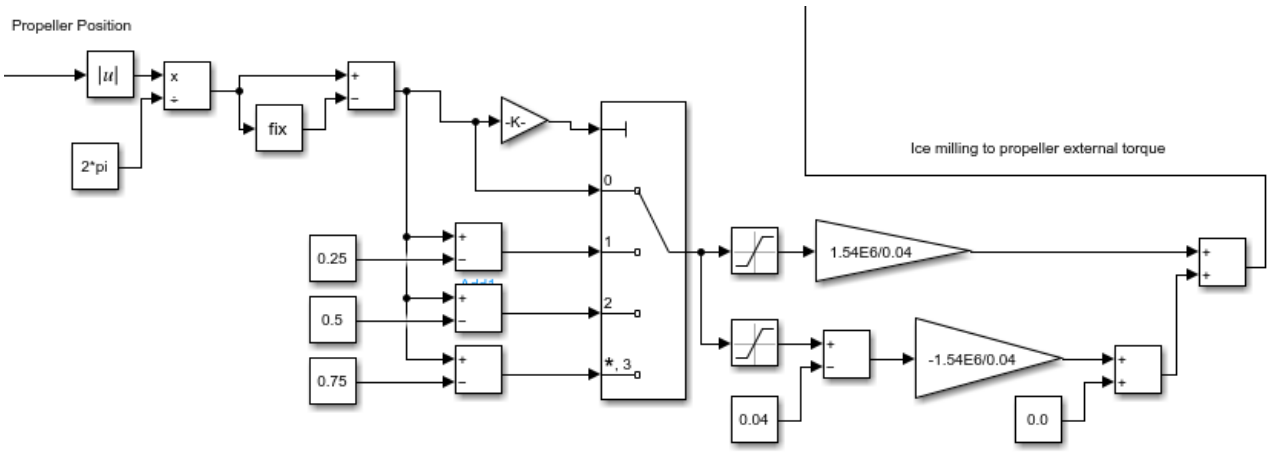

Figure 13. Ice milling external torque model.

3. Results

The aforementioned physical model described includes the major components of the electric generation, power conversion and propulsion systems, including the major diesel generator speed control governor, diesel engine, synchronous generator, excitation system, rectifier circuit, DC-link, filter, inverter, controller, permanent magnet synchronous motor, shaft and propeller. The external dynamics such as hull resistance and ice milling torque have also been accounted for. All of these components/subsystems were modeled at a level of complexity consistent models found in the literature and the goals of this initial analysis. Future studies may warrant higher-fidelity and complexity models depending on the study objectives.

3.1. Ahead Operation

The simplest and perhaps most frequent maneuvering operation is the ahead command (Figure 14). During this evolution the shaft is initially motionless. A two second delay period is included to allow the generator excitation system to stabilize and build voltage in the DC-link. At t = 2 s the desired shaft speed set point is ramped up from 0 RPM to 143 RPM. In this scenario the hull, propeller and shaft dynamics are all set for open water operation, with the propeller torque coefficient varying with shaft and vessel speed. At t = 25 s the speed demand reaches its final value, though steady state shaft speed takes an additional 10 s to achieve due to system inertia. The motor phase current I_a is sinusoidal with frequency and magnitude varying as commanded by the controller to match the desired shaft speed amid the variable external torque.

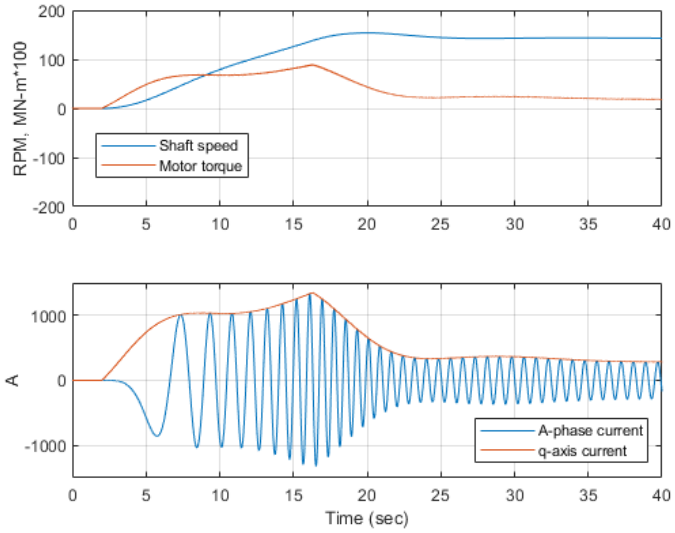

Figure 14. Ahead operation as calculated with the Healy end-to-end model.

The system appears to be functioning as expected for this type of operation, with higher currents drawn by the motor during system acceleration, where inertial torques are significant, with the current decreasing during steady-state operation, where motor torque is needed to overcome bearing and propellor hydraulic drag. Total harmonic distortion of the current was calculated to be less than 1%, demonstrating that harmonically, SPWM-type vector control is superior than use of a Cycloconverter-type motor drive.

3.2. Harmonic Distortion

A major advantage of utilizing a PWM drive over the Cycloconverter drive of the Healy is the potential reduction of harmonic currents in the propulsion motor power cables and windings. Harmonic have the effects of reducing torque and efficiency. The harmonic effect of the rectifier on the generator outputs appears to be relatively minor, as is the effect of the load on the PMSM, propagating back to the generator as an electrical load through the motor drive.

3.3. Ice Breaking

When the vessel encounters ice the open water resistance curves are no longer valid. For this test the same speed command timing is used as for the ahead test but the desired speed is increased to 143 RPM and the time range is expanded to 65 s in order to give the simulation adequate time for the ship's propulsion system to develop sufficient thrust to counter the increased hull resistance imposed by the ice.

This test was of relatively short duration, but sufficient to demonstrate the effect of ice breaking at steady state. As can be seen from Figure 15, the PMSM motor currents reach

their maximum value before the speed set point is reached. This analysis demonstrates stable operation during ice breaking.

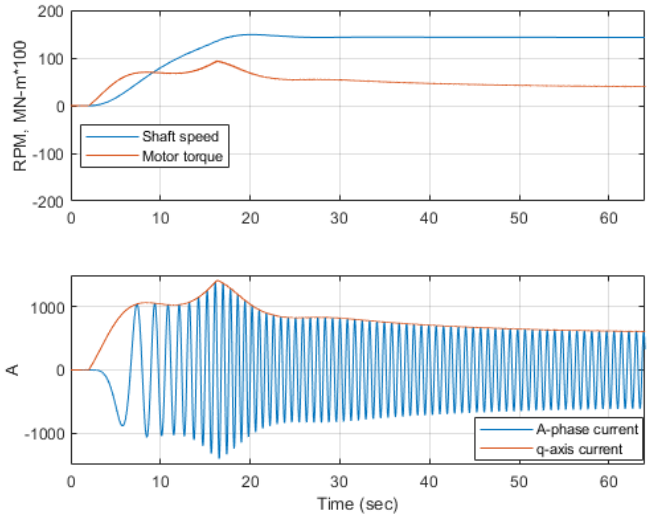

Figure 15. Motor current performance during ice breaking scenario.

3.4. Ice Milling

Ice milling is considered to be one of the more challenging operational scenarios for ice capable ships with PWM drives. The primary concern of this technology is whether the system can maintain stable motor drive and system control, and reject the substantial disturbance of ice milling loads.

The ice milling scenario assumes the vessel starts with a slow astern command of −38 RPM (−4 rad/s), followed by ice—impact and resultant milling. This is a likely scenario for a ship maneuvering in ice to change direction. Hydrostatic hull and propeller resistance, derived from Reference [2], are also included in this analysis.

The speed response, shown in blue in Figure 16, demonstrates the initial speed response from the moment the slow astern bell is given. The desired shaft speed is achieved in 3 s before the ice-milling torque (shown in red), is applied. Both speed and torque are shown as negative, indicating reverse operation.

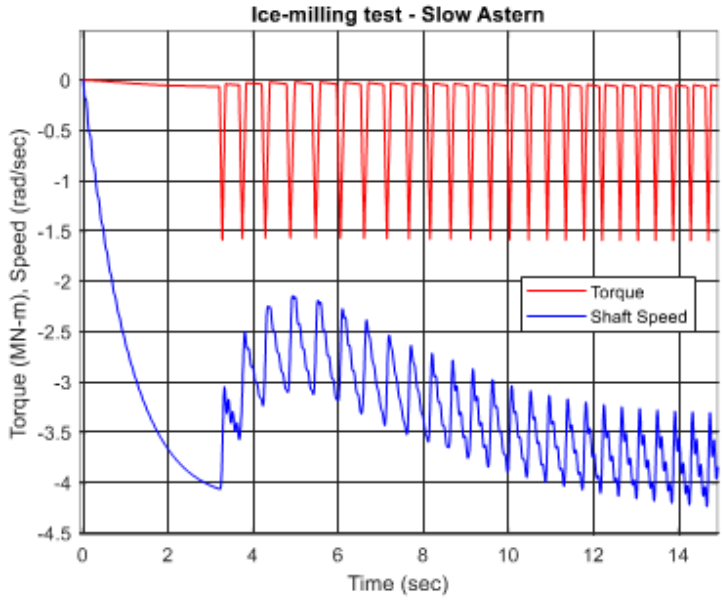

Figure 16. Ice Milling Shaft Speed and Torque—Slow Astern Operation.

It is clear that the initial torque has the effect of dramatic speed reduction. The system has been disturbed, clearly and repeatedly, causing additional speed reduction up to t = 5 s. However, despite the consistent, repetitive external torque loads, the propulsion motor recovers and corrects to achieve the desired speed set point. Steady state response is achieved despite continuous transient disruption from the external ice milling torque pulses.

As previously discussed, dq PMSM proportional-plus-integral control maintains $i_d = 0$ (or very close to it during transients). i_q is controlled to the demand value calculated by the motor speed controller (also proportional-plus-integral control). The i_d and i_q currents are shown in Figure 17 was observed during the same test run, shown below:

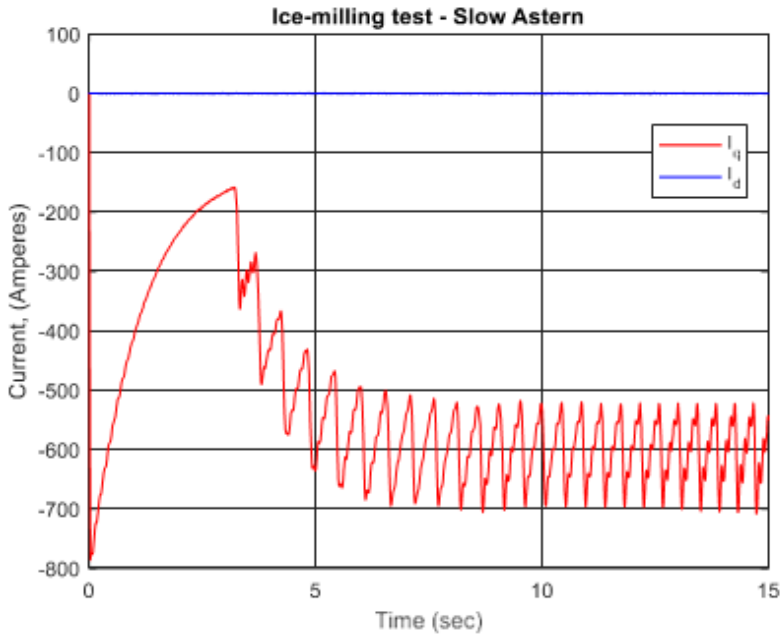

Figure 17. Ice milling motor dq currents.

As shown in Figure 17, i_d is effectively controlled to zero. i_q is effectively controlled to zero, and i_q performs as expected and is responsible for motor torque production. There is an initial current spike on the speed initial speed command that slowly fades as the desired shaft speed is reached. This is followed by more spikes as speed drops off due to external torque disturbance. Eventually, a semblance of steady state is achieved, but with repeating transient disruption from the continued, repetitive ice milling torque.

3.5. Crash Back (Emergency Crash Astern)

Although not necessary for ice breaking or ice milling, ship builder sea trials usually typically include an emergency astern test or "crash back" test at sea. To simulate this test the model was initialized with an initial hull velocity of 8 m/s in the ahead direction with throttle command at 143 RPM (15 rad/s). At t = 10 s a −143 RPM (full reverse) throttle command is given. The results of this test run are shown in Figure 18.

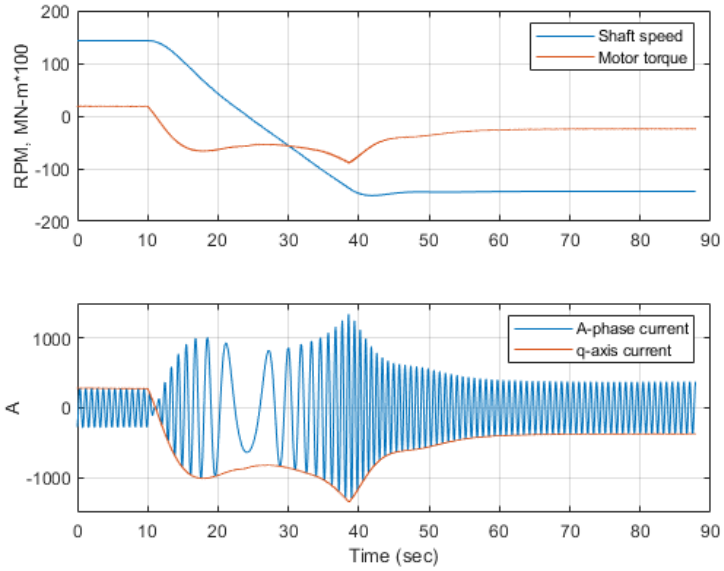

Figure 18. Motor performance during crash back test.

The USCGC Healy specification calls for a full power reversal within 25 s. Maximum Torque was achieved within this range, however the shaft speed continued to accelerate until more than 35 s after the reverse command was given in response to the hull dynamics. At t = 15 s after the full-astern command is given, a reversal is observed, as expected, in the A-phase and i_q currents (i_q should be the amplitude of the phase current) resulting is a change in the direction of shaft rotation. The shaft speed ultimately achieved the demanded −143 RPM, the torque performance is acceptable given that this maneuver would rarely, if ever, be encountered by this type of vessel.

4. Discussion

The results of this preliminary study demonstrate that a PWM-based inverter and dq current controller supplying power to a PMSM is a technically viable option for ice-capable vessel propulsion systems. The performance test simulations achieve stable operation throughout the load range, and successfully reject the most severe forms of external torque disruption that are expected to be encountered in typical ice service.

Moreover, the motor currents are shown to be sinusoidal during the different test conditions simulated unlike those of a cycloconverter motor drive. The reduced harmonic distortion allows the PMSM to be utilized most efficiently as demonstrated in the performance test results for the maneuvers analyzed. The notional PMSM chosen for the study is a 3-phase, surface-mounted machine, similar to those found in other ship propulsion applications, yet significantly different than the cycloconverter-based drive deployed on the Healy. In addition to the harmonic benefits of sine-triangle pulsed-width modulation over cycloconverter drives, application of PMSM provide for shipboard installations that are considerably more power-dense, smaller volume, and lighter weight than a wound-field, cycloconverter-fed synchronous motors.

The characterization of any operational savings available from the superior performance and the potential costs associated with the alternate equipment was outside of the scope of this analysis. As with any new design, these factors should be considered during the initial development phases.

Author Contributions: Conceptualization, E.C.R. and J.T.; methodology, E.C.R. and J.T.; software, E.C.R. and J.T.; validation, E.C.R. and J.T.; formal analysis, E.C.R. and J.T.; investigation, E.C.R.; resources, E.C.R. and J.T.; data curation, E.C.R.; writing—original draft preparation, E.C.R.; writing—review and editing, E.C.R. and J.T.; visualization, E.C.R. and J.T.; supervision, J.T.; project administration, J.T. All authors have read and agreed to the published version of the manuscript.

Funding: This research received no external funding.

Data Availability Statement: Data provided upon request.

Conflicts of Interest: The authors declare no conflict of interest.

References

1. John, A. Beverley, Chapter VIII Electric Propulsion Drives. In *Marine Engineering*; Roy, L.H., Ed.; Society of Naval Architects and Marine Engineers: Jersey City, NJ, USA, 1992.
2. Ned, M. *Electric Machines and Drives, A First Course*; John Wiley & Sons, Inc.: Hoboken, NJ, USA, 2012.
3. Lecourt, E.J., Jr. Using Simulation to Determine the Maneuvering Performance of the WAGB-20. *Nav. Eng. J.* **1998**, *110*, 171–188. [CrossRef]
4. Krause, W.; Sudhoff, P. *Analysis of Electric Machinery and Drive Systems*, 3rd ed.; Wiley: Hoboken, NJ, USA, 2013.
5. Chester, L. Long, Chapter X Propellers, Shafting, and Shafting System Vibration Analysis. In *Marine Engineering*; Roy, L.H., Ed.; Society of Naval Architects and Marine Engineers: Jersey City, NJ, USA, 1992.